Supplementary Materials

1 Optimization of extraction conditions

1.1 Investigation of methanol concentration

As illustrated in Fig. 4(a), the highest extraction yield of osthole was achieved at a methanol concentration of 70%. When the methanol concentration fell below 70%, the osthole yield showed a significant reduction, which was attributed to the excessively high polarity of the solvent. Conversely, when methanol concentration exceeded 70%, the extraction yields progressively decreased with increasing methanol concentration. This phenomenon likely resulted from reduced cell permeability caused by high methanol concentration, thereby inducing cellular dehydration and diminishing solvent extraction efficiency. Therefore, the optimal methanol concentration of 70% was identified and utilized for subsequent optimization experiments.

1.2 Investigation of extraction time

As illustrated in Fig. 4(b), the osthole extraction yield initially rose with prolonged extraction time but subsequently declined after reaching a peak. The maximum yield was observed at 1 hour, beyond which extended extraction time led to a reduction in osthole content, likely attributed to molecular degradation under prolonged thermal exposure. Therefore, an extraction duration of 1 hour was optimized and adopted for subsequent experimental iterations.

1.3 Investigation of solid to liquid ratio

As illustrated in Fig. 4(c), the extraction yield of osthole initially increased with the liquid-to-solid ratio but subsequently declined, reaching its maximum at a ratio of 6:1. This phenomenon can be attributed to the impaired mass transfer capacity caused by excessively high solvent volumes, which ultimately diminished the extraction yield. Therefore, a liquid-to-solid ratio of 6:1 was identified as optimal and adopted for subsequent process optimization.

1.4 Investigation of temperature

As illustrated in Fig. 4(d), the extraction yield of osthole exhibited an initial increase followed by a gradual decline, peaking at 70 °C. When the temperature was lower than

70 ℃, osthole extraction remained incomplete due to insufficient solubility. Above 70 ℃, thermal degradation of osthole and volatilization of solvent likely occurred, resulting in diminished extraction efficiency. Therefore, 70 ℃ was determined as the optimal temperature parameter for subsequent process optimization.

1.5 Investigation of extraction times

As illustrated in Fig. 4(e), the yield of osthole decreased gradually with the increase in extraction times. Repeated extraction processes likely induced osthole degradation in Cnidium monnieri fruits, resulting in reduced extraction efficiency. Given that Since the maximum extraction yield was achieved with a single extraction cycle, all subsequent experiments were conducted under this optimized parameter.

2. Analysis of variance(ANOVA)

The analysis of variance (ANOVA) revealed that the model exhibited a highly significant P-value ($p < 0.0001$). The lack-of-fit term showed a P-value of 0.3862 ($p > 0.05$), demonstrating no significant lack of fit and confirming the model's validity in explaining the experimental data. The coefficient of determination (R^2=0.9628) was 0.9628 demonstrated high consistency between experimental observations and model predictions. The adjusted R-squared (R^2Adj = 0.9256) indicated that 92.56% of the variation in osthole extraction could be accounted for by these four variables, confirming the model's predictive accuracy. With a coefficient of variation (CV=14.14%) below the 15% threshold, the experimental process demonstrated excellent repeatability and stability.

3. Analysis of pairwise interaction results

The interaction coefficient between liquid-to-solid ratio and methanol concentration was larger, which demonstrated a higher magnitude, suggesting these two variables exerted a more pronounced influence on the extraction process. In contrast, other interaction terms exhibited flatter profiles in the three-dimensional response surface plots, reflecting their minimal impact on the osthole extraction yield.

4. Supporting figures

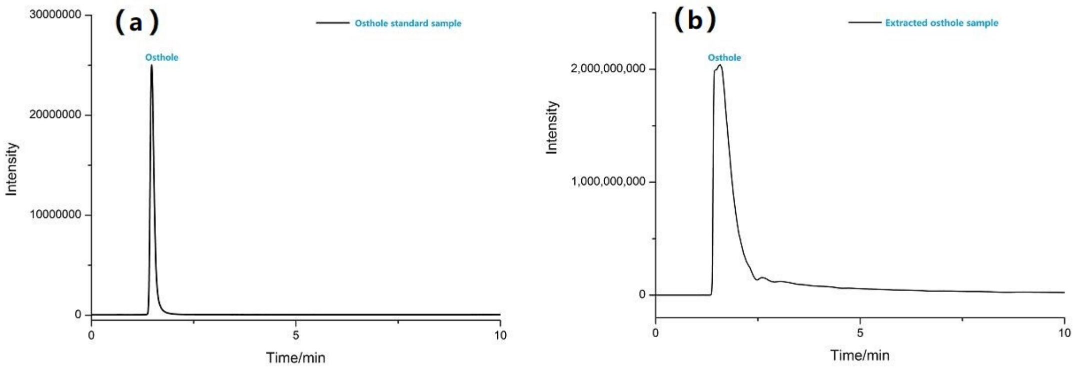

Fig. S1. Total ion chromatogram(TIC) of osthole standard sample (a) and extracted osthole sample(b)

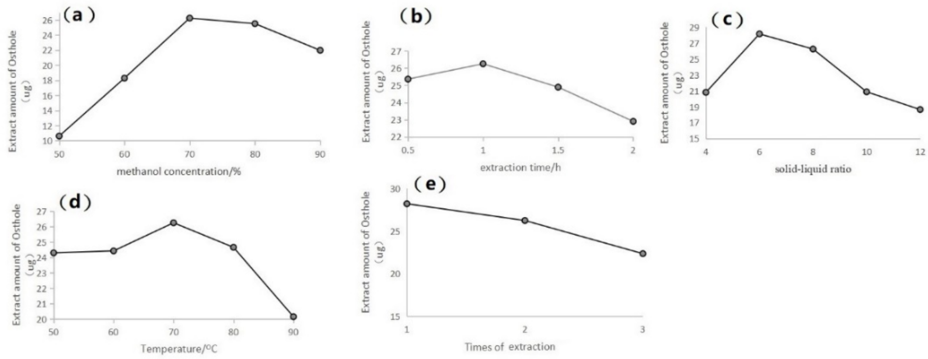

Fig. S2. Effect of parameter interactions on osthole extraction yield: (a) extraction time vs liquid-solid ratio, (b) extraction time vs temperature, (c) extraction time vs methanol concentration, (d) liquid-solid ratio vs temperature, (e) liquid-solid ratio vs methanol concentration, (f) temperature vs methanol concentration.

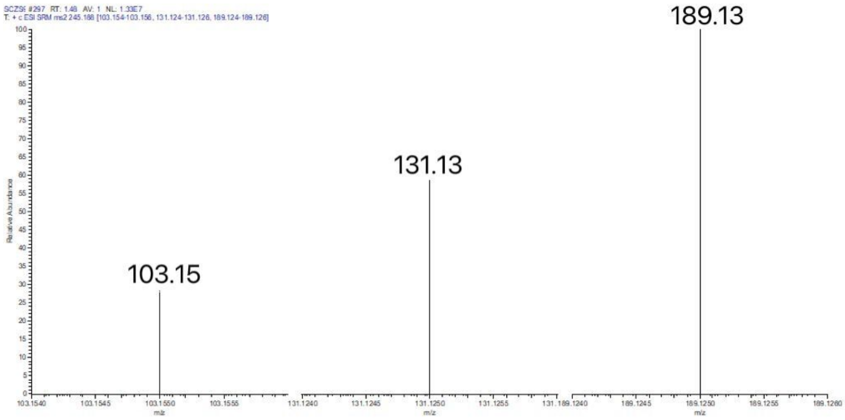

Fig. S3. Mass spectrometry analysis of osthole

5 Supporting tables

Table S1. Specifications of analytical apparatus

Apparatus	**Type**	**Manufacture**
Thermostatic Magnetic Stirrer	DF-101S	Kier (Wuhan, China)
Circulating water pumps Equipment	SHZ-D (III)	., Ltd. Zhengzhou north and south
Ultraviolet spectrophotometer	TU-1901	Persee (Beijing, China)
Rotary Evaporator	RE-52AA	Yarong (Shanghai, China)
HPLC-MS	TSQ Quantiva	Thermo Fisher (Waltham, American)
Octadecylsilyl (C18)	4.6mm，4.6×200mm 1.7 um，2.1×100mm	Elite Thermo Fisher scientific

Table S2. Chromatographic conditions and mass spectrometry parameters

Chromatographic condition		Mass spectrometry condition	
Separation Column	C_{18}（1.7 um，2.1×100mm）	Ion source	Electrospray
Mobile phase	water-methanol（20:80 , V:V）	Scanning mode	Positive ion
Flow rate	0.2 mL/min	Detection mode	MRM
Column temperature	40 ℃	Scanning Range	m/z 220→80
Injection volume	10 uL	Ionization voltage	3.40 KV

Table S3. Result of intra-day precision experiment

Number of experiments	Peak area of osthole（mAU）	Average peak area（mAU）	RSD %
1	3050.84	3144.53	1.91%
2	3131.16		
3	3127.53		
4	3150.12		
5	3174.04		
6	3233.52		

*n=3

Table S4. Result of inter-day precision experiment

Results	Days			Average Peak area of osthole	RSD%
	Day1	Day2	Day3		
Peak area of osthole（mAU）	4786.05	4753.11	4895.24	4811.47	1.546%

*n=3